Gold(I) halide complexes of bis(diphenylphosphine)diphenyl ether ligands: a balance of ligand strain and non-covalent interactions†

David V. Partyka,[a] James B. Updegraff III,[b] Matthias Zeller,[c] Allen D. Hunter[c] and Thomas G. Gray*[b]

Received 5th October 2009, Accepted 13th April 2010
First published as an Advance Article on the web 6th May 2010
DOI: 10.1039/b920717a

A series of bis(gold(I) halide; halide = Cl, Br, I) complexes of di(phosphino)diphenyl ether derivatives (L = DPEphos, DBFphos, Xantphos, tBuXantphos) have been synthesized. The new complexes have been characterized by X-ray crystallography, multinuclear NMR, and elemental analysis. The compounds luminesce at room temperature in dichloromethane solution. Many such complexes undergo aurophilic Au···Au bonding, and have chiral structures as a result. In complexes of the tBuXantphos ligand, X-ray crystallography indicates that an ion pair forms where the diphosphine ligand chelates one gold atom, and the other is part of an $[AuX_2]^-$ counterion (X = Cl, Br, I). It appears that the observed conformations of the metal-coordinated ligands are a balance of ligand strain and non-covalent interactions, including aurophilicity, intramolecular π-stacking, halide-halide repulsion, and intramolecular Au–O interactions. Together with previous investigations, this research shows that Xantphos and its derivatives form a robust set of coordination complexes with gold that are stable in air and amenable to further synthetic manipulation. It is anticipated that these materials will be suitable precursors for gold-carbon coupling reactions and gold-based catalysis.

Introduction

The semiflexible spacer 9,9-dimethylxanthene and others like it recur widely in ligands that support catalysis. These moieties act as connecting pillars in the pacman- and hangman-type porphyrins of Nocera and co-workers.[1–7] Diphosphine derivatives of xanthene[8,9] have use in rhodium-catalyzed hydroformylations,[10–16] cross-couplings,[17–20] and carbon-heteroatom bond formations.[21–25] The prototype diphosphine of this ligand set is Xantphos:

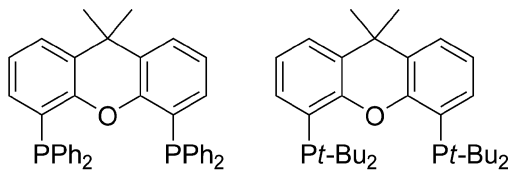

Molecular mechanics optimizations find Xantphos to have a bite angle of 108°. The bite of the *tert*-butyl derivative is wider, at 140°.[8]

Xantphos and related ligands bind transition elements primarily as macrochelates. In complexes of gold(I), their bidenticity opens access to hydridogold(I) cations.[26,27] Previously, these gold(I) hydrides had only been accessed in condensed phases with *N*-heterocyclic carbenes as supporting ligands.[28]

Gold(I) frequently adopts linear, two-coordinate binding geometries.[29–45] Two-coordinate gold(I) appears in several structurally authenticated diphosphine complexes of Xantphos and similar ligands.[46] Where steric hindrance is not great, aurophilic interactions occur. These are the attractive gold-gold interactions that dominate the structural chemistry of gold(I).[47–49] When aurophilic interactions happen in (diphosphine)gold(I) complexes, the resulting structures often lack improper rotations and are chiral.[50] At least one investigation has demonstrated solvent-assisted spontaneous resolution in chiral gold(I) diphosphine complexes.[51]

We have shown that gold(I) σ-organometallics are readily made from arylboronic acids and pinacolboronate esters.[39,42,44] The gold(I) reagents of choice are (phosphine) and (*N*-heterocyclic carbene)gold(I) bromides. We seek to explore the effects of π-stacking on gold aryls joined by a semirigid phosphine bridge. Accordingly, we are examining arylgold(I) complexes of Xantphos and similar ligands. We detail here the syntheses and structural characterization of precursors.

There are relatively few gold(I) complexes of Xantphos and kindred ligands, and they are gaining use in gold-based catalysis.[26,27,52] We have applied a convenient, biphasic synthesis protocol[53] that produces bromo analogues of (phosphine)gold chlorides.[54] We here show that this method extends to iodides, and that bromo and iodo variants of DPEphos-, DBFphos-, Xantphos-, and tBuXantphos-ligated gold(I) halide complexes in good to excellent yields.

Compounds are enumerated in Chart 1.

Experimental section

All solvents and reagents were used as received. DPEphos$(AuCl)_2$, DBFphos$(AuCl)_2$, and Xantphos$(AuCl)_2$ were synthesized by a slight modification of the literature procedure[46] (used toluene).

[a]*Creative Chemistry L.L.C., Cleveland, Ohio, 44106, USA*
[b]*Departments of Chemistry, Case Western Reserve University, Cleveland, Ohio, 44106, USA. E-mail: tgray@case.edu*
[c]*Youngstown State University, 1 University Plaza, Youngstown, Ohio, 44555, USA*

† Electronic supplementary information (ESI) available: Thermal ellipsoid depictions of **8** and **9**. CCDC reference numbers 750030, 750031, 750032, 750033, 750034, 750035, 750036, 750037 and 750038 for **1–9**. For ESI and crystallographic data in CIF or other electronic format see DOI: 10.1039/b920717a

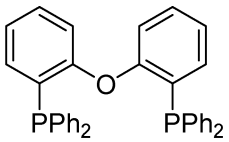

DPEphos

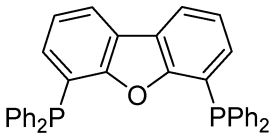

DBFphos

[DPEphos(AuBr)$_2$]	**1**
[DPEphos(AuI)$_2$]	**2**
[DBFphos(AuBr)$_2$]	**3**
[DBFphos(AuI)$_2$]	**4**
[Xantphos(AuBr)$_2$]	**5**
[Xantphos(AuI)$_2$]	**6**
[(tBuXantphosAu)(AuCl$_2$)]	**7**
[(tBuXantphosAu)(AuBr$_2$)]	**8**
[(tBuXantphosAu)(AuI$_2$)]	**9**

Chart 1 Designation of Ligands and Complexes.

All procedures were done in air, except for the synthesis of **7**. Microanalyses (C, H, and N) were performed by Quantitative Technologies Inc. NMR spectra (^{1}H and ^{31}P{^{1}H}) were recorded on a Varian AS-400 spectrometer. For ^{1}H and ^{31}P{^{1}H} NMR spectra, chemical shifts were determined relative to the solvent residual peaks. Emission spectra were collected in dichloromethane at room temperature on ~2×10^{-6} M samples that had been saturated with argon for at least 20 min.

[DPEphos(AuBr)$_2$] (1)

In 80 mL of dichloromethane was dissolved DPEphos(AuCl)$_2$ (424 mg. 0.42 mmol), and to this solution was added 14 equiv potassium bromide (704 mg, 5.9 mmol) in 50 mL of water. The mixture was stirred 4 h, at which point the organic layer was separated. Dichloromethane (20 mL) was added to extract the aqueous layer, and the organic layers were combined. The combined dichloromethane layers were washed twice with water (20 mL), and dried with $MgSO_4$. The organic layer was filtered, reduced to dryness by rotary evaporation, triturated with pentane, and the solid was collected and air-dried. Yield: 356 mg (77%). ^{1}H NMR ($CDCl_3$): δ 7.07–7.60 (m, 26H), 6.68 (ddd, 2H, J = 1.2, 7.6, 11.6 Hz) ppm. ^{31}P{^{1}H} NMR ($CDCl_3$): δ 23.6 (s) ppm. UV-Vis (dichloromethane): λ (ε, M^{-1} cm^{-1}) 285 (93000) nm. Anal. Calcd. for $C_{36}H_{28}Au_2Br_2OP_2 \cdot CH_2Cl_2$: C, 37.74; H, 2.57. Found: C, 37.28; H, 2.36.

[DPEphos(AuI)$_2$] (2)

In 100 mL of dichloromethane was dissolved DPEphos(AuCl)$_2$ (406 mg. 0.40 mmol), and to this solution was added 14 equiv potassium iodide (930 mg, 5.6 mmol) in 50 mL of water. The mixture was stirred 4 h, at which point the organic layer was separated. Dichloromethane (20 mL) was added to extract the aqueous layer, and the organic layers were combined. The combined dichloromethane layers were washed twice with water (20 mL), and dried with $MgSO_4$. The organic layer was filtered, reduced to dryness by rotary evaporation, and triturated with pentane to yield a white solid, which was collected and air-dried. Yield: 356 mg (97%). ^{1}H NMR ($CDCl_3$): δ 7.11–7.60 (m, 26H), 6.68 (dd, 2H, J = 7.6, 10.4 Hz) ppm. ^{31}P{^{1}H} NMR ($CDCl_3$): δ 27.9 (s) ppm. UV-Vis (dichloromethane): λ (ε, M^{-1} cm^{-1}) 285 (125000) nm. Anal. Calcd. for $C_{36}H_{28}Au_2I_2OP_2 \cdot CH_2Cl_2$: C, 34.95; H, 2.38. Found: C, 35.53; H, 1.96.

[DBFphos(AuBr)$_2$] (3)

In 100 mL of dichloromethane was dissolved DBFphos(AuCl)$_2$ (302 mg, 0.30 mmol), and to this solution was added potassium bromide (14 equiv, 503 mg, 4.2 mmol) dissolved in 50 mL of water. The biphasic mixture was stirred for 4 h, and the organic layer separated and retained. The aqueous layer was extracted once with dichloromethane (20 mL), and combined with the previously separated organic layer. The combined organic layers were washed twice with distilled water (20 mL), dried with magnesium sulfate, and filtered. The filtrate was reduced to dryness *via* rotary evaporation, and triturated with pentane. After soaking in pentane for several hours, the solid was collected and dried. An analytically pure sample was obtained by diffusion of pentane vapor into a saturated 1,2-dichloroethane solution of **3**. Yield: 290 mg (88%). ^{1}H NMR ($CDCl_3$): δ 8.18 (d, 2H, J = 8.0 Hz), 7.44–7.62 (m, 20H), 7.41 (td, 2H, J = 1.2, 8.0 Hz), 7.08 (ddd, 2H, J = 1.2, 7.6, 12.8 Hz) ppm. ^{31}P{^{1}H} NMR ($CDCl_3$): δ 26.8 (s) ppm. UV-Vis (dichloromethane): λ (ε, M^{-1} cm^{-1}) 285 (109000) nm. Anal. Calcd. for $C_{36}H_{26}Au_2Br_2OP_2 \cdot C_2H_4Cl_2$: C, 38.38; H, 2.37. Found: C, 37.71; H, 1.97.

[DBFphos(AuI)$_2$] (4)

In 25 mL of dichloromethane was dissolved DBFphos(AuCl)$_2$ (50 mg, 0.050 mmol), and to this solution was added 14 equiv potassium iodide (116 mg, 0.70 mmol) in 20 mL of water. The mixture was stirred 4 h, at which point the organic layer was separated. Dichloromethane (20 mL) was added to extract the aqueous layer, and the organic layers were combined. The combined dichloromethane layers were washed twice with water (10 mL), and dried with $MgSO_4$. The organic layer was filtered, reduced to dryness by rotary evaporation, triturated with pentane, and the solid was collected and dried. Recrystallization by vapor diffusion of pentane into a saturated chloroform solution caused separation of a colorless crystalline mass. The product has some sensitivity to light in $CDCl_3$ solution. Yield: 40 mg (68%). ^{1}H NMR ($CDCl_3$): δ 8.18 (d, 2H, J = 8.0 Hz), 7.44–7.60 (m, 20H), 7.42 (td, 2H, J = 1.2, 8.0 Hz), 7.14 (ddd, 2H, J = 1.2, 7.6, 12.8 Hz) ppm. ^{31}P{^{1}H} NMR ($CDCl_3$): δ 29.4 (s) ppm. UV-Vis (dichloromethane): λ (ε, M^{-1} cm^{-1}) 285 (95000) nm. Anal. Calcd. for $C_{36}H_{26}Au_2I_2OP_2$: C, 36.51; H, 2.21. Found: C, 36.34; H, 2.13.

[Xantphos(AuBr)$_2$] (5)

In 100 mL of dichloromethane was dissolved XantPhos(AuCl)$_2$ (370 mg, 0.36 mmol), and to this solution was added 14 equiv potassium bromide (591 mg, 5.0 mmol) in 50 mL of water.

The mixture was stirred 4 h, at which point the organic layer was separated. Dichloromethane (20 mL) was added to extract the aqueous layer, and the organic layers were combined. The combined dichloromethane layers were washed twice with water (20 mL), and dried with $MgSO_4$. The organic layer was filtered, reduced to dryness by rotary evaporation, triturated with pentane, and the solid was collected and dried. The solid has sensitivity to light. Yield: 380 mg (95%). ^{1}H NMR ($CDCl_3$): δ 7.63 (d, 2H, J = 7.6 Hz), 7.18–7.44 (m, 18H), 7.06 (t, 4H, J = 8.4 Hz), 6.46 (dd, 2H, J = 7.6, 11.6 Hz), 1.68 (s, 6H, CH_3) ppm. ^{31}P{^{1}H} NMR ($CDCl_3$): δ 24.3 (s) ppm. UV-Vis (dichloromethane): λ (ε, M^{-1} cm^{-1}) 284 (102000) nm. Anal. Calcd. for $C_{39}H_{32}Au_2Br_2OP_2$: C, 41.37; H, 2.85. Found: C, 41.75; H, 2.77.

[Xantphos(AuI)$_2$] (6)

In 60 mL of dichloromethane was dissolved XantPhos(AuCl)$_2$ (170 mg, 0.16 mmol), and to this solution was added 14 equiv potassium bromide (370 mg, 3.1 mmol) in 30 mL of water. The mixture was stirred 4 h, at which point the organic layer was separated. Dichloromethane (20 mL) was added to extract the aqueous layer, and the organic layers were combined. The combined dichloromethane layers were washed twice with water (20 mL), and dried with $MgSO_4$. The organic layer was filtered and reduced to dryness by rotary evaporation. The solid-residue was triturated with pentane and the solid collected and dried. Yield: 179 mg (90%). ^{1}H NMR ($CDCl_3$): δ 7.62 (d, 2H, J = 8.0 Hz), 7.18–7.44 (m, 18H), 7.07 (t, 4H, J = 8.0 Hz), 6.48 (dd, 2H, J = 8.0, 10.8 Hz), 1.68 (s, 6H, CH_3) ppm. ^{31}P{^{1}H} NMR ($CDCl_3$): δ 24.0 (s) ppm. UV-Vis (dichloromethane): λ (ε, M^{-1} cm^{-1}) 284 (127000) nm. Anal. Calcd. for $C_{39}H_{32}Au_2I_2OP_2$: C, 38.20; H, 2.63. Found: C, 38.26; H, 2.46.

[(tBuXantphosAu)(AuCl$_2$)] (7)

In 3 mL of toluene in a glove box was dissolved tBuXantphos (62 mg, 0.12 mmol) and this solution was added dropwise to a suspension of tetrahydrothiophenegold(I) chloride (2 equiv, 80 mg, 0.25 mmol) in 3 mL of toluene. Over the course of several minutes the mixture became a white suspension. After 12 h stirring, the solvent was removed by rotary evaporation, and the residue was triturated with pentane. The white solid was collected and dried. Yield: 118 mg (99%). ^{1}H NMR ($CDCl_3$): δ 7.77 (d, 2H, J = 7.6 Hz), 7.65–7.70 (m, 2H), 7.46 (t, 2H, J = 7.6 Hz), 1.66 (s, 6H, CH_3), 1.50–1.60 (m, 36H, C(CH_3)$_3$) ppm. ^{31}P{^{1}H} NMR ($CDCl_3$): δ 69.2 (s) ppm. UV-Vis (dichloromethane): λ (ε, M^{-1} cm^{-1}) 285 (115000) nm. Anal. Calcd. for $C_{31}H_{48}Au_2Cl_2OP_2$: C, 38.64; H, 5.02. Found: C, 38.38; H, 4.81.

[(tBuXantphosAu)(AuBr$_2$)] (8)

In 10 mL of dichloromethane was dissolved **7** (58 mg, 0.06 mmol), and to this solution was added 12 equiv potassium bromide (92 mg, 7.7 mmol) in 10 mL of water. The mixture was stirred 4 h, at which point the organic layer was separated. Dichloromethane (15 mL) was added to extract the aqueous layer, and the organic layers were combined. The combined dichloromethane layers were washed twice with water (15 mL), and dried with $MgSO_4$. The organic layer was filtered, reduced to dryness by rotary evaporation and triturated with pentane. The white solid was collected and dried. Yield: 43 mg (68%). ^{1}H NMR ($CDCl_3$): δ 7.76 (dd, 2H, J = 1.6, 7.6 Hz), 7.63–7.68 (m, 2H), 7.45 (t, 2H, J = 7.6 Hz), 1.64 (s, 6H, CH_3), 1.48–1.54 (m, 36H, C(CH_3)$_3$) ppm. ^{31}P{^{1}H} NMR ($CDCl_3$): δ 69.5 (s) ppm. UV-Vis (dichloromethane): λ (ε, M^{-1} cm^{-1}) 285 (95000) nm. Anal. Calcd. for $C_{31}H_{48}Au_2Br_2OP_2$: C, 35.38; H, 4.60. Found: C, 35.34; H, 4.48.

[(tBuXantphosAu)(AuI$_2$)] (9)

In 25 mL of dichloromethane was dissolved **7** (124 mg, 0.13 mmol), and to this solution was added 14 equiv potassium iodide (305 mg, 1.8 mmol) in 20 mL of water. The mixture was stirred 4 h, at which point the yellow organic layer was separated. Dichloromethane (10 mL) was added to extract the aqueous layer, and the organic layers were combined. The combined dichloromethane layers were washed twice with water (15 mL), and dried with $MgSO_4$. The organic layer was filtered, reduced to dryness by rotary evaporation and triturated with pentane. The yellow solid was collected and dried. Yield: 132 mg (89%). ^{1}H NMR ($CDCl_3$): δ 7.76 (dd, 2H, J = 1.6, 7.6 Hz), 7.63–7.68 (m, 2H), 7.44 (t, 2H, J = 7.6 Hz), 1.64 (s, 6H, CH_3), 1.48–1.55 (m, 36H, C(CH_3)$_3$) ppm. ^{31}P{^{1}H} NMR ($CDCl_3$): δ 69.2 (s) ppm. UV-Vis (dichloromethane): λ (ε, M^{-1} cm^{-1}) 280 (108000) nm. MS (ES^-): Calcd. m/z = 450.7755 $(AuI_2)^-$; Found m/z = 450.7755. MS (ES^+): Calcd. m/z = 695.2846 $(LAu)^+$; Found m/z = 695.2849. Anal. Calcd. for $C_{31}H_{48}Au_2I_2OP_2$: C, 32.48; H, 4.22. Found: C, 32.75; H, 4.15.

X-ray crystallography

Crystals of **9** were grown by layering a saturated ~2 : 1 ether/acetonitrile solution with pentane, while all other crystals were grown by vapor diffusion of pentane into saturated chloroform solutions. Single crystals of **6** sufficed only to determine connectivity; data are included as Supporting Information.† Single crystal X-ray data were collected on a Bruker AXS SMART APEXII CCD diffractometer using monochromatic Mo-Kα radiation with omega scan technique. The unit cells were determined using APEX2 Crystallographic Suite. All structures were solved by direct methods and refined by full matrix least squares against F^2 with all reflections using SHELXTL. Refinement of extinction coefficients was found to be insignificant. All non-hydrogen atoms were refined anisotropically. All other hydrogen atoms were placed in standard calculated positions and all hydrogen atoms were refined with an isotropic displacement parameter 1.5 (CH_3) or 1.2 (all others) times that of the adjacent carbon atom. Crystallographic data for **1–9** appear in Tables 1 and 2.

Results and discussion

Synthesis

Our approach to these diphosphine gold bromides and iodides[7] begins with the synthesis of the chlorinated analogues, which are known except for **7**, the tBuXantphos derivative.[46] Product **7** was easily synthesized by treating a suspension of two equivalents of Au(tht)Cl (tht = tetrahydrothiophene) in toluene with one equivalent of tBuXantphos (as a toluene solution) in a glovebox. The air stable product (an ion pair) precipitates from toluene and can be collected using standard procedures.[54] The air- and water-stable bromo and iodo analogues are prepared from the chloro

Table 1 Crystallographic Data for Diphosphine Gold(I) Halides **1–5**

	1	**2**	**3**	**4**	**5**
Formula	$C_{36}H_{28}Au_2Br_2OP_2 \cdot CHCl_3$	$C_{36}H_{28}Au_2I_2OP_2 \cdot CHCl_3$	$C_{36}H_{26}Au_2Br_2OP_2$	$C_{36}H_{26}Au_2I_2OP_2$	$C_{39}H_{32}Au_2Br_2OP_2$
fw	1211.65	1305.63	1090.26	1184.24	1132.34
cryst syst	Monoclinic	Monoclinic	Triclinic	Monoclinic	Monoclinic
Space group	$P2_1/c$	$P2_1/c$	$P\bar{1}$)	$P2_1/n$	$P2_1/n$
a/Å	8.981(3)	9.0814(13)	12.0279(19)	9.5702(9)	10.5328(19)
b/Å	20.448(7)	20.656(3)	12.491(2)	19.0596(18)	18.360(3)
c/Å	19.993(7)	20.934(3)	12.561(2)	19.3026(18)	19.185(4)
α (°)	—	—	109.152(2)	—	—
β (°)	102.957(5)	102.566	92.054(2)	103.1610(10)	96.391(2)
γ (°)	—	—	94.291(2)	—	—
cell volume/Å^3	3578(2)	3832.8(10)	1774.1(5)	3428.4(6)	3687.1(12)
Z	4	4	2	4	4
D_c/Mg m^{-3}	2.249	2.263	2.041	2.294	2.040
T/K	100(2)	100(2)	100(2)	100(2)	100(2)
μ/mm^{-1}	10.769	9.579	10.629	10.471	10.232
F(000)	2272	2416	1016	2176	2128
cryst size, mm^3	0.21 × 0.18 × 0.06	0.20 × 0.18 × 0.06	0.21 × 0.11 × 0.06	0.40 × 0.14 × 0.10	0.37 × 0.10 × 0.10
θ_{min}, θ_{max} (°)	1.00, 28.28	0.99, 28.28	1.70, 26.99	1.52, 28.99	1.54, 26.91
no. of reflns collected	28618	36368	20142	41518	33682
no. of indep reflns	6440	9613	6515	7591	6188
no. of refined params	425	419	388	388	417
goodness-of-fit on F^2[a]	1.031	1.142	1.115	1.043	1.009
Final R indices [b] $[I > 2\sigma(I)]$ R_1	0.0813	0.0461	0.0332	0.0255	0.0512
wR_2	0.1223	0.0533	0.0385	0.0561	0.0667
R indices (all data) R_1	0.1749	0.1025	0.0988	0.0291	0.1331
wR_2	0.1974	0.1060	0.1007	0.0573	0.1416

[a] GOF = $[\sum w(F_o^2 - F_c^2)^2/(n-p)]^{1/2}$; n = number of reflections, p = number of parameters refined. [b] $R_1 = \sum(\|F_o| - |F_c\|)/\sum|F_o|$; $wR_2 = [\sum w(F_o^2 - F_c^2)^2/\sum wF_o^4]^{1/2}$.

Table 2 Crystallographic Data for **7–9**

	7	**8**	**9**
Formula	$C_{31}H_{48}AuOP_2 \cdot AuCl_2$	$C_{31}H_{48}AuOP_2 \cdot AuBr_2$	$C_{31}H_{48}AuOP_2 \cdot AuI_2$
Fw	963.47	1052.39	1146.37
cryst syst	Triclinic	Triclinic	Triclinic
Space group	$P\bar{1}$	$P\bar{1}$	$P\bar{1}$
a/Å	7.7838(6)	7.8004(15)	7.9986(4)
b/Å	13.1896(10)	13.229(3)	13.4430(7)
c/Å	16.5684(13)	16.615(3)	16.9930(9)
α (°)	80.6320(10)	80.764(2)	80.9230(10)
β (°)	82.7010(10)	83.754(2)	83.9480(10)
γ (°)	83.3990(10)	83.867(2)	84.2300(10)
cell volume/Å^3	1656.5(2)	1675.3(6)	1787.68(16)
Z	2	2	2
D_c/Mg m^{-3}	1.932	2.086	2.130
T/K	296(2)	100(2)	296(2)
M, mm^{-1}	9.127	11.250	10.035
F(000)	928	1000	1072
cryst size, mm^3	0.50 × 0.22 × 0.14	0.49 × 0.37 × 0.11	0.21 × 0.16 × 0.15
θ_{min}, θ_{max} (°)	1.25, 28.28	1.57, 27.04	1.22, 28.28
no. of reflns collected	16901	18664	18279
no. of indep reflns	7367	6652	7864
no. of refined params	357	357	357
goodness-of-fit on F^2[a]	1.087	1.021	1.135
Final R indices [b] $[I > 2\sigma(I)]$ R_1	0.0247	0.0333	0.0213
wR_2	0.0288	0.0358	0.0264
R indices (all data) R_1	0.0636	0.1201	0.0507
wR_2	0.0755	0.1241	0.0615

[a] GOF = $[\sum w(F_o^2 - F_c^2)^2/(n-p)]^{1/2}$; n = number of reflections, p = number of parameters refined. [b] $R_1 = \sum(\|F_o| - |F_c\|)/\sum|F_o|$; $wR_2 = [\sum w(F_o^2 - F_c^2)^2/\sum wF_o^4]^{1/2}$.

complexes by a simple biphasic procedure (reactions 1 and 2) in isolated yields ranging from 68–97%.

$$L(AuCl)_2 + \text{excess KBr (aq)} \rightarrow L(AuBr)_2 \quad (1)$$

$$L(AuCl)_2 + \text{excess KI (aq)} \rightarrow L(AuI)_2 \quad (2)$$

NMR spectroscopy

^{1}H and ^{31}P NMR spectra were measured for all new compounds in $CDCl_3$. Common to the ^{1}H NMR spectra of **1–6** and in analogy with chloro precursors, a low-frequency aromatic resonance that appears as a doublet of doublet of doublets or doublet of doublets is assigned as an *ortho*-H resonance of the aryl ether rings, in agreement with Lagunas.[46] The protons of the diphenylphosphino fragments appear as a multiplet, and in the case of the rigid Xantphos backbones of **5–9**, diagnostic methyl resonances appear as singlets near 1.65 ppm.

^{31}P NMR was especially useful in determining both identity and purity of products. As has been shown previously, ^{31}P chemical shifts are sensitive to the ligand *trans* to phosphorus in phosphine-ligated gold(I) halide complexes, at parity of phosphine.[54,55] Table 3 collects these data.

The data show that this sensitivity to *trans*-disposed ligand reappears in non-rigid gold complexes of DPEphos and the rigid gold complexes of DBFphos, but not the Xantphos derivatives. It is unclear why this should be the case, but it may result from a conformationally rigid xanthene backbone or a strong aurophilic interaction that may exist in solution. The ^{31}P chemical shift of **3** is insensitive to the halide ligand, possibly because neighboring

Table 3 Observed ^{31}P NMR Chemical Shifts δ (ppm) for Aurated Diphosphine Complexes[a]

Diphosphine	δ ^{31}P (X = Cl)	δ ^{31}P (X = Br)	δ ^{31}P (X = *I*)
DPEphos	21.7	23.6	27.9
DBFphos	25.2	26.8	29.4
Xantphos	24.0	24.0	24.3
tBuXantphos	69.2	69.5	69.2

[a] All chemical shifts reported in $CDCl_3$.

gold atoms are too far apart for aurophilic contact. The crystal structure shows gold atoms more than 7 Å apart, *vide infra.* In the case of the tBuXantphos derivatives **7–9**, a cation-anion pair of the type (diphosphine-Au)$^+$(AuX$_2$)$^-$ forms, so regardless of the identity of halide, the cation is little affected, and ^{31}P chemical shifts are nearly unchanging.

UV-visible and emission spectroscopy

All complexes except **9** are colorless in the solid state (**9** is yellow, even when recrystallized); however, in solution products **1–9** have similar absorption spectra in dichloromethane. In the high energy direction, absorption begins around 350 nm and maximizes around 285 nm. Absorption is likely due to $\pi \rightarrow \pi^*$ transitions, with the lowest energy transition expected to involve the diphenyl ether motif common to all products. In contrast to the fine structure observed in solid state absorption spectra of the chloro analogues,[46] no fine structure appears in the absorption spectra of **1–9** in solution. However, when excited at the lowest energy region of absorptivity (~330 nm), fine structure in the emission of **1–9** was observed.

X-ray crystallography

Complexes **1–9** have been characterized by single crystal X-ray diffraction. The most notable feature of these complexes is the binding geometry at gold, which is two-coordinate and linear for **3**, two-coordinate with gold-gold bonding for **1**, **2**, and **4–6**; and two-coordinate quasi-linear and cationic for the ion pairs **7–9**. The ligand diphenyl ether backbone for each aurated product twists and accommodates strain. The amount of "twist" induced in the diphenyl ether backbone is conveniently described by the torsion angle P1-C$_{ipso1}$-C$_{ipso2}$-P2 (φ_1). In addition to the torsion angle φ_1, all products with a gold-gold interaction are described by two other torsion angles, φ_2 (P1-Au1-Au2-P2) and φ_3 (X1-Au1-Au2-X2) (angles are illustrated in Scheme 1; for φ_1 the perspective is down the axis connecting C$_{ipso1}$ and C$_{ipso2}$ and for $\varphi_{2,3}$ the perspective is down the Au–Au axis). All relevant data appear in Table 4. Fig. 1 shows thermal ellipsoid representations of the DPEphos derivatives **1** and **2**.

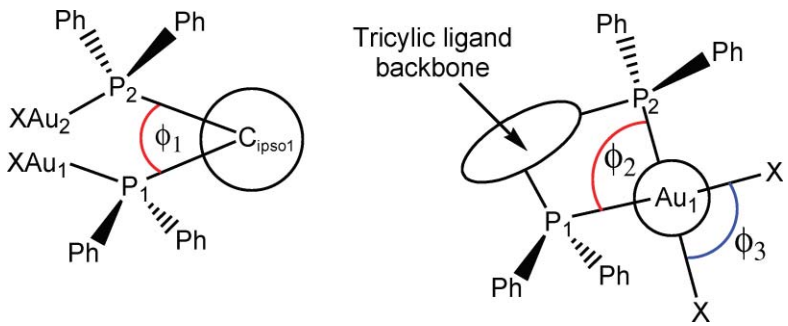

Scheme 1

Table 4 Geometric Parameters for Crystallographically Characterized Products

	Au–Au/Å	Shortest Au–O/Å	Shortest Intramolecular π-Stacking Distance/Å	P–P/Å	θ/°	φ_1 (°)	φ_2 (°)	φ_3 (°)
DPEphos[a]	—	—	3.610	4.876	—	63.5	—	—
DPEphos(AuCl)$_2$[a]	3.0038(6)	3.496	3.561	4.858	—	2.8	81.8	80.9
1	2.9764(13)	3.442	3.544	4.913	—	59.1	82.2	84.0
2	2.9857(7)	3.454	3.538	4.927	—	58.5	80.7	82.1
DBFphos[b]	—	—	3.609	5.741(1)	177.3	5.0	—	—
DBFphos(AuCl)$_2$[a]	>7.2	3.990	3.490	5.834	177.4	21.1	—	—
3	>7.2	3.615	3.463	5.897	174.5	18.8	—	—
4	3.1528(3)	3.139	[f]	5.365	178.5	6.9	66.1	91.0
Xantphos[c,d,e]	—	—	3.486, 3.445, 3.650	4.045(1), 4.059, 4.155(1)	156.6, 156.2, 159.9	0.0, 0.0, 0.8	—	—
Xantphos(AuCl)$_2$[a]	2.9947(4)	3.097	3.742	4.735	150.3	39.4	87.1	90.7
5	2.9233(6)	3.090	3.628	4.656	154.5	37.4	85.6	88.0
6	2.892(2)	3.069	3.641	4.620	154.2	36.6	84.8	89.8
tBuXantphos	—	—	—	4.180	179.4	2.2	—	—
7	>5.7	2.659	—	4.487	143.0	13.7	—	—
8	>5.7	2.660	—	4.479	142.5	11.7	—	—
9	>6.0	2.672	—	4.497	143.0	9.0	—	—

[a] Values taken from reference 46 and data therein. [b] Values taken from reference 10. [c] Values taken from references 58a,b. [d] Listed values are for three polymorphs of the crystallized ligand. [e] Third value in each box is for Xantphos·THF. [f] Undefined because of disorder in one phosphine phenyl group.

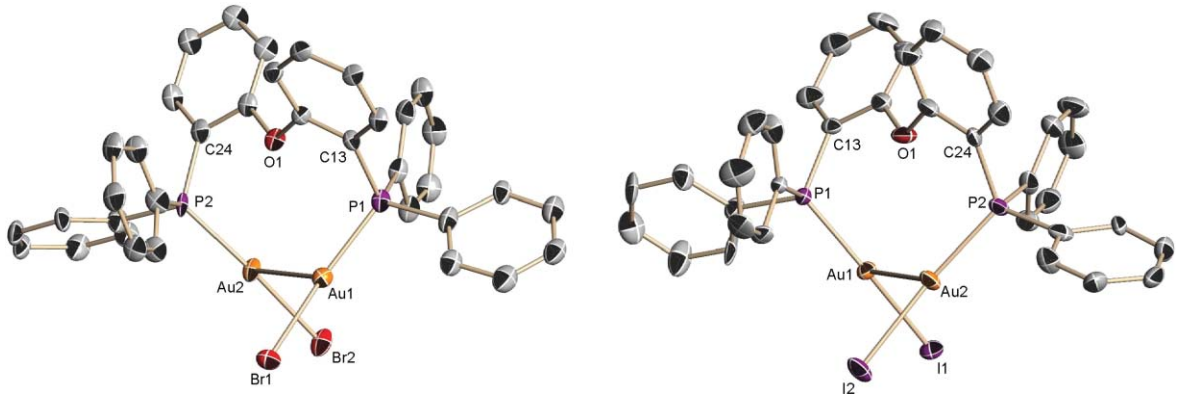

Fig. 1 Thermal ellipsoid representation of the *R*-enantiomer of **1** (left) and the *R*-enantiomer of **2** showing 50% probability ellipsoids and partial atom-labeling scheme. Hydrogen atoms and a chloroform molecule of co-crystallization have been omitted for clarity. Selected bond distances (Å) and bond angles (°) (**1**): Au1-Au2, 2.9764(13); Au1-P1, 2.234(5); Au2-P2, 2.233(5); Au1-Br1, 2.400(2); Au2-Br2, 2.414(2). P1-Au1-Br1, 166.24(15); P2-Au2-Br2, 174.32(14); P1-Au1-Au2, 100.98(14); Br1-Au1-Au2, 92.50(6); P2-Au2-Au1, 105.44(13); Br2-Au2-Au1, 80.17(6). (**2**): Au1-Au2, 2.9857(7); Au1-P1, 2.256(3); Au2-P2, 2.268(3); Au1-I1, 2.5748(8); Au2-I2, 2.5893(8). P1-Au1-I1, 167.06(7); P2-Au2-I2, 171.24(8); P1-Au1-Au2, 99.39(7); I1-Au1-Au2, 93.20(3); P2-Au2-Au1, 107.18(7); I2-Au2-Au1, 81.43(2).

The DPEphos ligand supports two-coordinate gold(I) with an aurophilic contact. The gold-halogen and gold-phosphorus distances for **1** and **2** are unexceptional, and the short gold-gold distances for both products indicate a strong aurophilic interaction.[47] To achieve these conformations, the ligand has twisted considerably, as indicated by torsions $\varphi_1 = 54°$ and 59° for **1** and **2** (*e.g.*, P1-C13-C24-P2 for **2**) respectively. The torsion angles φ_3 are 84° and 82°, compared to 81° in the chloro analogue.[46] Since all of three members of the series (X = Cl, Br, I) have similar torsion angles φ_3, and all are virtually identical except for coordinating different terminal halides, which bear negative charge, it is conceivable that φ_3 represents the optimum balance between maximizing halide distance *versus* minimizing ligand conformational strain. At distances of greater than 3.45 Å, the Au–O distances are too far to consider any substantial interaction. However, both **1** and **2** possess aryl carbon atoms on one-half of the molecule that appear to π-stack with aryl carbon atoms on the opposite half of the molecule; these distances are approximately 3.54 Å for both **1** and **2** (compared to approximately 3.56 Å and 3.61 Å respectively[46]), and may also contribute to the solid-state conformation.

The DBFphos analogues of **1** and **2** have also been crystallographically characterized, and thermal ellipsoid representations appear as Fig. 2. Compound **3** is similar to its chlorinated analogue in that the distance between gold atoms is too far (greater than 7.2 Å) for direct gold-gold interaction. In a bis(phenylacetylenegold(I)) analogue of **3**, the distance between gold atoms is 3.401(1) Å,[56] which is short enough to consider a weak aurophilic interaction. It is tempting to suppose that the bite angle of the DBFphos ligand is too large to support anything but a weak gold-gold interaction, especially since the crystallographically determined solid-state conformations of DBFphos,[57] DBFphos(AuCl)$_2$, and **3** appear to be reinforced by intramolecular phenyl ring π–π stacking interactions (C–C distances of closest approach less than 3.5 Å in each case). However, the structure of **4** proves that DBFphos can support a somewhat short gold-gold interaction. The flexibility of the DBFphos ligand becomes clear upon considering the P–P distances in **3** and **4**, which are approximately 5.90 Å and 5.37 Å respectively, compared to the P–P distance in free DBFphos, which is 5.741(1) Å. Inspection of Table 4 clearly indicates that **4** is an exception to the rule in the fused tricyclic ring diphosphine complexes **3–9** (and in chlorinated

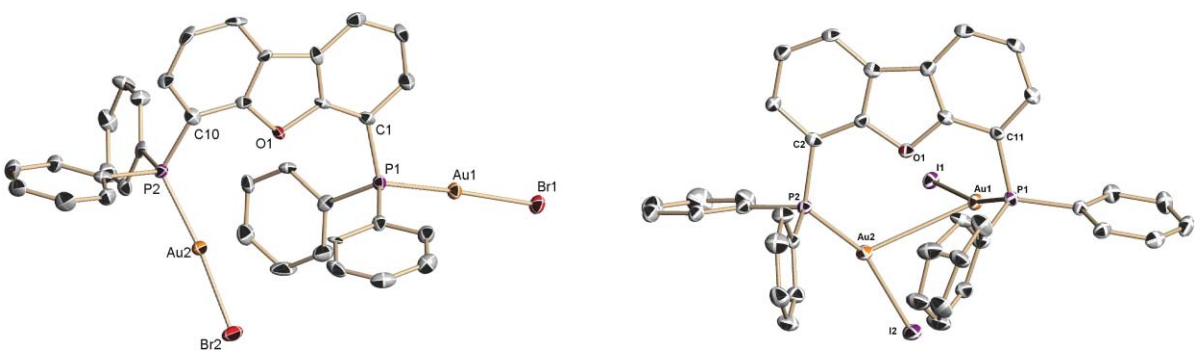

Fig. 2 Thermal ellipsoid representation of **3** (left) and the *R*-enantiomer of **4** showing 50% probability ellipsoids and partial atom-labeling scheme. Hydrogen atoms have been omitted for clarity. Selected bond distances (Å) and bond angles(°) (**3**): Au1-P1, 2.229(2); Au2-P2, 2.230(2); Au1-Br1, 2.4071(11); Au2-Br2, 2.4043(10); 2.3761(8). P1-Au1-Br1, 167.63(6); P2-Au2-Br2, 171.58(6); P1-Au1-Au2, 95.58(5); Br1-Au1-Au2, 95.64(2); P2-Au2-Au1, 100.99(5); Br2-Au2-Au1, 82.97(2). (**4**): Au1-Au2, 3.1528(3); Au1-P1, 2.2532(11); Au2-P2, 2.2526(11); Au1-I1, 2.5745(4); Au2-I2, 2.5775(4). P1-Au1-I1, 164.99(3); P2-Au2-I2, 158.81(3); P1-Au1-Au2, 107.86(3); I1-Au1-Au2, 76.142(9); P2-Au2-Au1, 116.89(3); I2-Au2-Au1, 82.078(11).

derivatives), as metal coordination in all other complexes *increases* the P–P distances.

The angles P–C_{ipso}-$C_{ring\ fusion}$ measure 124.9(4)° (P1-C1-C12) and 124.3(5)° (P2-C10-C11) *versus* 121.4(4)° (P1-C2-C1) and 117.0(4)° (P2-C11-C12) for **3** and **4** respectively. The torsion angle φ_1 measures 21°, 19° and 7° for DBFphos$(AuCl)_2$, **3** and **4** respectively, indicating that the ligand backbone is not severely distorted in any case. Since **4** has a gold-gold interaction, the torsion angles φ_2 and φ_3 are informative, and measure 66° and 91° respectively. The comparatively large value for φ_3 again suggests that maximizing the halide-halide distance is a contributing factor to the observed molecular conformation. A comparison of the angles P–Au-X in **3** *versus* **4** shows that this angle is more acute in the latter, which is expected since the aurophilic contacts of **4** induce a slight trigonalization at gold.

Fig. 3 shows a thermal ellipsoid representation of **5**; that of **6** appears as Supporting Information.† The bond lengths at gold are unexceptional, and the Au1-Au2 distance indicates a strong aurophilic interaction. As in **1**, **2**, and **4**, the aurophilic interactions impose a quasi-trigonal geometry at Au1 and, along with a sub-van der Waals contact between Au2 and O1 (approximately 3.09 Å), quasi-four coordination at Au2. The fold angle θ (illustrated in Scheme 2), defined as the angle of intersection between the mean planes containing each C_6 Xantphos phenyl ring is approximately 155°, very similar to the value observed for the three different reported crystal structures of free Xantphos (angles range from 156–160°).[58] However, the similarities between the free diphosphine and the metal-coordinated diphosphine end here. Inspection of Table 4 indicates that metal coordination causes considerable distortion of the Xantphos ligand. The torsion angle φ_1 measures approximately 0°, 39°, 37°, and 37° for Xantphos, Xantphos$(AuCl)_2$, **5**, and **6** respectively, suggesting that the Xantphos ligand better tolerates torsional strain than does DBFphos (both with respect to the long axis of the ligand). The likely reason is the unsaturated CMe_2 unit connecting the diphenyl ether backbone. Furthermore, the

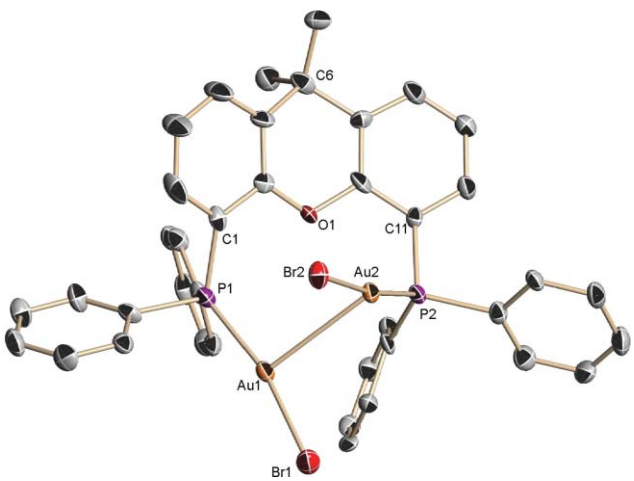

Fig. 3 Thermal ellipsoid representation of the *R*-enantiomer of **5** showing 50% probability ellipsoids and partial atom-labeling scheme. Hydrogen atoms have been omitted for clarity. Selected bond distances (Å) and bond angles(°) (**5**): Au1-Au2, 2.9233(6); Au1-P1, 2.229(2); Au2-P2, 2.230(2); Au1-Br1, 2.4071(11); Au2-Br2, 2.4043(10); 2.3761(8). P1-Au1-Br1, 167.63(6)(5); P2-Au2-Br2, 171.58(6); P1-Au1-Au2, 95.58(5); Br1-Au1-Au2, 95.64(2); P2-Au2-Au1, 100.99(5); Br2-Au2-Au1, 82.97(2).

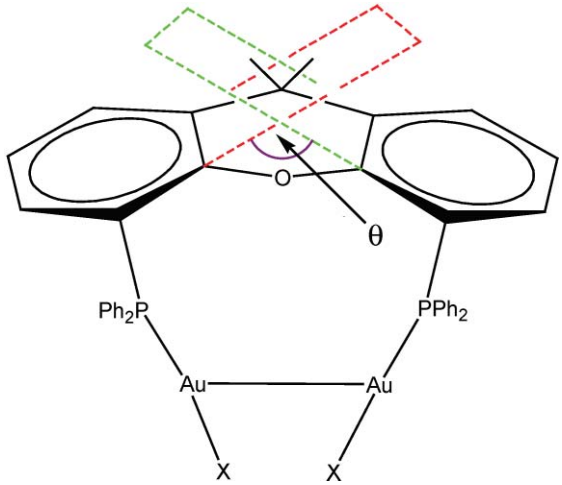

Scheme 2

P–P distance increases by ~0.5–0.7 Å upon metal coordination. In the asymmetric unit, only one enantiomer is present, however, two enantiomers of each helical configuration are present in the centrosymmetric unit cell ($P2_1/n$). Clearly, in the solid state P1 and P2 are in different chemical environments, so the fact that only one phosphorus singlet is observed in the ^{31}P NMR spectrum (*vide supra*) implies that there is fast conversion between enantiomers in solution.

The ligand tBuXantphos, in contrast to the other diphosphine ligands, forms an ion pair [LAu][AuX_2] for all X = Cl, Br, and I. Compound **8** is representative, and a thermal ellipsoid projection appears as Fig. 4. The cationic fragment of each product **7–9** is very similar, thus discussion will focus on **8** (thermal ellipsoid representations of **7** and **9** are provided in Supporting Information as Figure S1 and S2 respectively†). All bond distances and angles for **8** are unexceptional save for the P1-P2 distance (4.479 Å, which is approximately 0.3 Å greater than free tBuXantphos[59]), and the angle P1-Au1-P2, which at 153.46(5)° is relatively acute for gold(I) (gold(I) generally features bond angles closer to 180° when two coordinate). However, this angle is near the bite angle of 153° observed in *trans*-(Xantphos)Pd(Me)Cl[60] and 151° observed for *trans*-(Xantphos)Pd(4-cyanophenyl)Br.[61]

Interestingly, in comparison to the Xantphos ligand of **5**, the central six-membered ring of the tBuXantphos ligand of **8** assumes a much more pronounced boat-like conformation (the dihedral angle formed by the planes defined by C1-O1-C13 and C6-C7-C8 is 111° *versus* 136° for the corresponding angle in **5**). In **8**, θ is approximately 143°. In contrast, in the crystal structure of free tBuXantphos,[59] the tBuXantphos tricyclic backbone is almost flat (fold angle equals ~180°); the central ring does not assume a boat-like conformation, and the P1-P2 distance is 4.180 Å, almost 0.3 Å smaller than in **8**. The Au1-Br1 distance (approximately 3.87 Å) is too far to indicate an interaction between the two atoms. The ^{31}P NMR data (*vide supra*) suggest that the solid state conformation of **7–9** is maintained in solution at room temperature, as only one singlet is observed. Interestingly and in contrast to **1–8**, complex **9** is yellow as the isolated solid even after recrystallization. However, once dissolved, **9** is spectroscopically identical to **7** and **8**, and mass spectrometry (in chloroform) shows the existence of discrete [tBuXantphosAu]$^+$ and [AuI_2]$^-$ ions in high abundance. This color

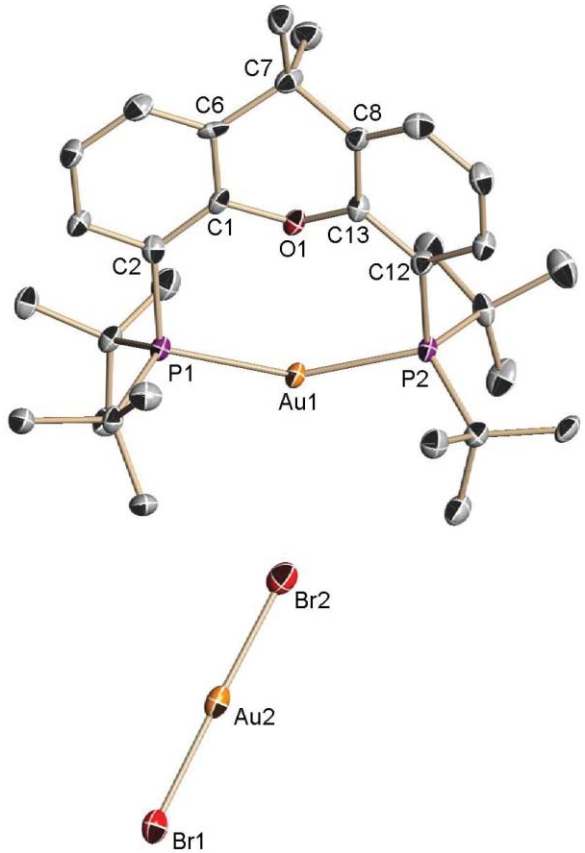

Fig. 4 Thermal ellipsoid drawing of **8** showing 50% probability ellipsoids and partial atom-labeling scheme. Hydrogen atoms have been omitted for clarity. Selected bonds distances (Å) and bond angles (°): Au1-P1, 2.3027(13); Au1-P2, 2.2993(13); Au2-Br1, 2.3736(8); Au2-Br2, 2.3761(8). P1-Au1-P2, 153.46(5); Br1-Au1-Br2, 178.68(2).

cannot be due to an impurity, as microanalysis of the isolated solid was nearly perfect. In addition, the color cannot be due to ligand to metal charge transfer transitions within the $[AuI_2]^-$ fragment, as the UV-visible spectrum of **9** is identical to the spectra of the chloro and bromo analogues in the same solvent (dichloromethane). It is possible that the distance between one iodide ligand and the gold cation (less than 4 Å) is close enough for an interionic ligand (iodide) to metal (gold cation) charge transfer in the solid state, but this evidence is not conclusive.

Discussion

It is not surprising that Xantphos and similar diphosphines support gold(I) bromide and gold(I) iodide fragments, considering reports by Lagunas and co-workers,[46] and many studies demonstrating that Xantphos derivatives bind metals across the transition series.[1–27] Chelation is most commonly observed, and the monodentate binding observed repeatedly in this investigation adds to the coordination chemistry of these ligands. However, the observation that tBuXantphos exclusively chelates gold and forms a gold(I) dihalide ion pair under identical reaction conditions indicates that the binding mode is a compromise of several factors. Although it is not very common, ligand redistribution to form ion pairs of the type $[ML_2]^+[MX_2]^-$ (L = two monodentate ligands or one bidentate ligand; X = halide) has been observed for both gold(I) and silver(I). In the case of gold(I), the phosphine diadamantylbenzylphosphine (Ad_2BnP) reacts with Au(tht)Cl to form an ion pair $[(Ad_2BnP)_2Au](AuCl_2)$ at room temperature,[62] whereas in the case of silver(I), various imidazolium halides react with silver oxide to form ion pairs of the type $[Ag(carbene)_2][AgX_2]$.[63–65]

Two of the most important factors dictating the mode of binding appear to be the flexibility of the diphosphine and a balance of non-covalent interactions. The non-covalent interactions include aurophilic interactions, intramolecular π-stacking, halide-halide repulsion, and weak Au–O interactions. This is illustrated by the contrast between **4** and its bromo and chloro analogues. As mentioned above, the crystallographically proven solid-state conformations of DBFphos,[10] DBFphos$(AuCl)_2$, and **3** appear to be reinforced by phenyl ring π–π stacking interactions (C–C distances of closest approach less than 3.5 Å in each case), however, in **4** it appears that stabilizing aurophilic interaction offsets the loss of stabilizing intramolecular π–π stacking interactions, as the π-stacking distance increases to nearly 3.77 Å. Furthermore, crystal packing effects (the space groups of DBFphos, DBFphos$(AuCl)_2$, **3**, and **4** are $P2_1/n$, $P2_1/c$, $P\bar{1}$, $P2_1/n$ respectively) and a hydrogen bonded diethyl ether of crystallization in DBFphos$(AuCl)_2$ may have some influence on the observed conformations in the solid state. The program Mercury[66] identifies several sub-van der Waals intermolecular contacts.

Several experimental observations attest to the flexibility of the diphenylphosphino ligands. For example, in the DBFphos series, the P–P distance for the free ligand, **3** and **4** are 5.74 Å, 5.90 Å, and 5.37 Å respectively, which indicates that the ligand flexes for the P–P distance to contract or expand. In the case of **4**, the contraction distance (relative to the free ligand) is not insignificant. In the Xantphos and tBuXantphos series of complexes, metal coordination increases the P–P distances by ~0.5–0.7 Å and ~0.3 Å respectively.

Another example of the flexibility of these ligands is found in the tBuXantphos series. The tricylic ring system of the free ligand is almost perfectly planar,[12] but the central ring of the chelated adducts **7–9** folds significantly along *two* perpendicular axes. Specifically, the boat conformation dihedral angle formed by the planes defined by C1-O1-C13 and C6-C7-C8 in product **8** is 111° (whereas it is nearly 180° in the free ligand), and the fold angle θ (*vide supra*) is approximately 143° (in the free ligand it is nearly 180°). The Xantphos derivative **5** displays similar central ring distortions, but not nearly of the same magnitude (the values for the boat conformation dihedral angle and the fold angle are approximately 136° and 155° respectively for **5**). The most obvious reason for the difference in magnitude of these angles is the short Au–O contact in **7–9** that is less significant in **5** (the Au–O distances are approximately 2.66 Å and 3.09 Å for **8** and **5** respectively). This conformation may also help minimize conjugation with the two phenyl rings, which would allow the oxygen atom to bind gold more effectively. However, a cationic Pd(II) complex, [*trans*-(Xantphos)Pd(4-cyanophenyl)](OTf), has a short Pd–O distance of 2.154 Å,[61] which suggests that this Au–O interaction may be comparatively weak. As before, inspecting the three-dimensional structures of **5** and **8** relative to the corresponding free ligands indicates that to accommodate the gold atom(s), the P–P distance has expanded by approximately 0.6 and 0.3 Å respectively. One possibility is that the bulkier tBuXantphos ligand does not

dilate the P–P distance enough to accommodate an aurophilic Au_2 pair.

Conclusions

Gold(I) chloride adducts of DPEphos and its derivatives, similar to mononuclear systems, have demonstrated their usefulness as precursors to more labile bromo and iodo analogues. In the case of tBuXantphos, the diphosphine ligand chelates one gold cation, and a gold dihalide counteranion balances charge. All complexes have been characterized by UV-visible, emission, and NMR spectroscopies in addition to X-ray crystallography. X-ray crystallography has ascertained that the rigid ligands DBFphos, Xantphos, and tBuXantphos are more flexible. For most complexes, binding accommodates short aurophilic pairings. The distortion of these ligands to accommodate the observed conformations and aurophilic interactions suggests that metal binding is strongly favored thermodynamically. We believe that these complexes will be synthetic precursors for the formation of a variety of organogold complexes, studies on which are ongoing.

Acknowledgements

We thank the U.S. National Science Foundation (grant CHE-0749086 to T. G. G.) for support. T. G. G. is an Alfred P. Sloan Foundation Fellow. The diffractometer at Case Western Reserve was funded by NSF grant CHE-0541766; that at Youngstown State University, by NSF grant 0087210, by the Ohio Board of Regents grant CAP-491, and by Youngstown State University. We thank N. Deligonul for assistance with crystallography.

References

1 J. Rosenthal and D. G. Nocera, *Prog. Inorg. Chem.*, 2007, **55**, 483and references therein .
2 J. Rosenthal and D. G. Nocera, *Acc. Chem. Res.*, 2007, **40**, 543.
3 C. J. Chang, E. A. Baker, B. J. Pistorio, Y. Deng, Z. -H. Loh, S. E. Miller, S. D. Carpenter and D. G. Nocera, *Inorg. Chem.*, 2002, **41**, 3102.
4 C. -Y. Yeh, C. J. Chang and D. G. Nocera, *J. Am. Chem. Soc.*, 2001, **123**, 1513.
5 C. J. Chang, L. -L. Chng and D. G. Nocera, *J. Am. Chem. Soc.*, 2003, **125**, 1866.
6 J. D. Soper, S. V. Kryatov, E. V. Rybak-Akimova and D. G. Nocera, *J. Am. Chem. Soc.*, 2007, **129**, 5069.
7 J. R. Rosenthal, L. -L. Chng, S. D. Fried and D. G. Nocera, *Chem. Commun.*, 2007, 2642.
8 M. -N. Birkholz, Z. Freixa and P. W. N. M. van Leeuwen, *Chem. Soc. Rev.*, 2009, **38**, 1099.
9 P. Dierkes and P. W. N. M. van Leeuwen, *J. Chem. Soc., Dalton Trans.*, 1999, 1519.
10 M. Kranenburg, Y. E. M. Van Der Burgt, P. C. J. Kamer, P. W. N. M. van Leeuwen, K. Goubitz and J. Fraanje, *Organometallics*, 1995, **14**, 3081.
11 R. P. J. Bronger, J. P. Bermon, J. Herwig, P. C. J. Kamer and P. W. N. M. van Leeuwen, *Adv. Synth. Catal.*, 2004, **346**, 789.
12 L. A. Van Der Veen, P. H. Keeven, G. C. Schoemaker, J. N. H. Reek, P. C. J. Kamer, P. W. N. M. van Leeuwen, M. Lutz and A. L. Spek, *Organometallics*, 2000, **19**, 872.
13 L. A. Van Der Veen, M. D. K. Boele, F. R. Bregman, P. C. J. Kamer, P. W. N. M. van Leeuwen, K. Goubitz, J. Fraanje, H. Schenk and C. Bo, *J. Am. Chem. Soc.*, 1998, **120**, 11616.
14 L. A. Van Der Veen, P. C. J. Kamer and P. W. N. M. van Leeuwen, *Angew. Chem., Int. Ed.*, 1999, **38**, 336.
15 R. P. J. Bronger, P. C. J. Kamer and P. W. N. M. van Leeuwen, *Organometallics*, 2003, **22**, 5358.
16 J. I. Van Der Vlugt, R. Sablong, P. C. M. M. Magusin, A. M. Mills, A. L. Spek and D. Vogt, *Organometallics*, 2004, **23**, 3177.
17 M. Kranenburg, P. C. J. Kamer and P. W. N. M. van Leeuwen, *Eur. J. Inorg. Chem.*, 1998, 155.
18 M. Carril, R. SanMartin, F. Churruca, I. Tellitu and E. Domínguez, *Org. Lett.*, 2005, **7**, 4787.
19 L. Wu and J. F. Hartwig, *J. Am. Chem. Soc.*, 2005, **127**, 15824.
20 J. -Y. Lee and P. H. Lee, *J. Org. Chem.*, 2008, **73**, 7413.
21 S. Deprèle and J. -L. Montchamp, *J. Am. Chem. Soc.*, 2002, **124**, 9386.
22 L. Coudray, K. Bravo-Altamirano and J. -L. Montchamp, *Org. Lett.*, 2008, **10**, 1123.
23 K. Bravo-Altamirano, I. Abrunhosa-Thomas and J. -L. Montchamp, *J. Org. Chem.*, 2008, **73**, 2292.
24 A. M. Johns, M. Utsunomiya, C. D. Incarvito and J. F. Hartwig, *J. Am. Chem.Soc.*, 2006, **128**, 1828.
25 V. V. Grushin and W. J. Marshall, *J. Am. Chem. Soc.*, 2006, **128**, 12644.
26 H. Ito, T. Saito, T. Miyahara, C. Zhong and M. Sawamura, *Organometallics*, 2009, **28**, 4829.
27 A Escalle, G. Mora, F. Gagosz, N. Mézailles, X. F. Le Goff, Y. Jean and P. Le Floch, *Inorg. Chem.*, 2009, **48**, 8415.
28 E. Y. Tsui, P. Müller and J. P. Sadighi, *Angew. Chem., Int. Ed.*, 2008, **47**, 8937.
29 H. E. Abdou, A. A. Mohammed and J. P. Fackler, Jr., in *Gold Chemistry: Applications and Future Directions*, F. Morh, Ed. Wiley, 2009, Chapter 1.
30 H. Schmidbaur and A. Schier, in *Comprehensive Organometallic Chemistry III*, R. Crabtree and M. Migos, ed., Elsevier, 2006, Volume 2, Section 2.05.
31 H. Schmidbaur, A. Grohmann and M. E. Olmos, in *Gold: Progress in Chemistry, Biochemistry and Technology*, H. Schmidbaur, Ed., Wiley, Chichester, 1999.
32 E. J. Fernández, A. Laguna and M. E. Olmos, *Adv. Organomet. Chem.*, 2004, **52**, 77.
33 J. P. Fackler, Jr., *Inorg. Chem.*, 2002, **41**, 6959.
34 T. G. Gray, *Comments Inorg. Chem.*, 2007, **28**, 181–212.
35 R. K. Arvapally, P. Sinha, S. R. Hettiarachchi, N. L. Coker, C. E. Bedel, H. H. Patterson, R. C. Elder, A. K. Wilson and M. A. Omary, *J. Phys. Chem. C*, 2007, **111**, 10689.
36 O. Elbjeirami and M. A. Omary, *J. Am. Chem. Soc.*, 2007, **129**, 11384.
37 D. S. Laitar, P. Müller, T. G. Gray and J. P. Sadighi, *Organometallics*, 2005, **24**, 4503.
38 D. V. Partyka, J. B. Updegraff III, M. Zeller, A. D. Hunter and T. G. Gray, *Organometallics*, 2007, **26**, 183.
39 D. V. Partyka, A. J. Esswein, M. Zeller, A. D. Hunter and T. G. Gray, *Organometallics*, 2007, **26**, 3279.
40 D. V. Partyka, T. J. Robilotto, M. Zeller, A. D. Hunter and T. G. Gray, *Proc. Natl. Acad. Sci. U. S. A.*, 2008, **105**, 14293.
41 D. V. Partyka, T. J. Robilotto, J. B. Updegraff, III, M. Zeller, A. D. Hunter and T. G. Gray, *Organometallics*, 2009, **28**, 795.
42 D. V. Partyka, J. B. Updegraff, III, M. Zeller, A. D. Hunter and T. G. Gray, *Organometallics*, 2009, **28**, 1666.
43 L. Gao, D. V. Partyka, J. B. Updegraff, III, N. Deligonul and T. G. Gray, *Eur. J. Inorg. Chem.*, 2009, 2711.
44 L. Gao, M. A. Peay, J. B. Updegraff, III, T. S. Teets, A. J. Esswein, M. Zeller, A. D. Hunter and T. G. Gray, *Organometallics*, 2009, **28**, 5669.
45 D. V. Partyka, M. P. Washington, T. G. Gray, J. B. Updegraff, III, J. F. Turner, II and J. D. Protasiewicz, *J. Am. Chem. Soc.*, 2009, **131**, 10041.
46 A. Pintado-Alba, H. de la Riva, M. Nieuwhuyzen, D. Bautista, P. R. Raithby, H. A. Sparkes, S. J. Teat, J. M. López-de Luzuriaga and M. C. Lagunas, *Dalton Trans.*, 2004, 3459.
47 H. Schmidbaur and A. Schier, *Chem. Soc. Rev.*, 2008, **37**, 1931.
48 H. Schmidbaur, *Gold Bull.*, 2000, **33**, 3.
49 A. L. Balch, *Gold Bull.*, 2004, **37**, 45.
50 F. A. Cotton, *Chemical Applications of Group Theory*, John Wiley and Sons, New York, 3rd edn, 1990, p. 34.
51 T. Tunyogi, A. Deák, G. Tárkányi, P. Király and G. Pálinkás, *Inorg. Chem.*, 2008, **47**, 2049.
52 H. Ito, K. Takagi, T. Miyahara and M. Sawamura, *Org. Lett.*, 2005, **7**, 3001.
53 D. Schneider, A. Schier and H. Schmidbaur, *Dalton Trans.*, 2004, 1995.
54 D. V. Partyka, T. J. Robilotto, M. Zeller, A. D. Hunter and T. G. Gray, *Organometallics*, 2008, **27**, 28.
55 D. V. Partyka, M. Zeller, A. D. Hunter and T. G. Gray, *Angew. Chem., Int. Ed.*, 2006, **45**, 8188.

56 H. de la Riva, M. Nieuwhuyzen, C. M. Fierro, P. R. Raithby, L. Male and M. C. Lagunas, *Inorg. Chem.*, 2006, **45**, 1418.
57 E. M. Vogl, J. Bruckmann, C. Krüger and M. W. Haenel, *J. Organomet. Chem.*, 1996, **520**, 249.
58 (*a*) S. Hillebrand, J. Bruckmann, C. Krüger and M. W. Haenel, *Tet. Lett.*, 1995, **36**, 75; (*b*) M. Kranenburg, Y. E. M. Van Der Burgt, P. C. J. Kamer, P. W. N. M. van Leeuwen, K. Goubitz and J. Fraanje, *Organometallics*, 1995, **14**, 3081.
59 C. Mispelaere-Canivet, J. -F. Spindler, S. Perrio and P. Beslin, *Tetrahedron*, 2005, **61**, 5253.
60 M. A. Zuideveld, B. H. G. Swennenhuis, Y. Guari, G. P. F. van Strijdonck, M. D. K. Boele, J. N. H. Reek, P. C. J. Kamer, K. Goubitz, J. Fraanje, M. Lutz, A. L. Spek and P. W. N. M. van Leeuwen, *J. Chem. Soc., Dalton Trans.*, 2002, 2308.
61 J. Yin and S. L. Buchwald, *J. Am. Chem. Soc.*, 2002, **124**, 6043.
62 U. Monkowius, M. Zabel and H. Yersin, *Inorg. Chem. Comm.*, 2008, **11**, 409.
63 P. de Frémont, N. M. Scott, E. D. Stevens, T. Ramnial, O. C. Lightbody, C. L. B. Macdonald, J. A. C. Clyburne, C. D. Abernethy and S. P. Nolan, *Organometallics*, 2005, **24**, 6301.
64 A. C. Sentman, S. Csihony, R. M. Waymouth and J. L. Hedrick, *J. Org. Chem.*, 2005, **70**, 2391.
65 H. M. J. Wang and I. J. B. Lin, *Organometallics*, 1998, **17**, 972.
66 Mercury CSD 2.2 (Build RC5). http://www.ccdc.cam.ac.uk/mercury/.